Atmospheric Environment 232 (2020) 117546

Contents lists available at ScienceDirect

Atmospheric Environment

journal homepage: http://www.elsevier.com/locate/atmosenv

Black carbon transport between Santiago de Chile and glaciers in the Andes Mountains

Ernesto Gramsch [a,*], Alicia Muñoz [b], Joakim Langner [c], Luis Morales [d], Cristian Soto [a], Patricio Pérez [a], María A. Rubio [e]

[a] Physics Department,University of Santiago de Chile, Av. Ecuador 3493, Santiago, Chile
[b] Ministry of the Environment, San Martín 73, Santiago, Chile
[c] Swedish Meteorological and Hydrological Institute, SE, 601 76, Norrköping, Sweden
[d] Faculty of Agronomic Sciences, University of Chile, Av. Santa Rosa N° 11315, Santiago, Chile
[e] Faculty of Chemistry, University of Santiago de Chile, Av. Ecuador 3493, Santiago, Chile

HIGHLIGHTS

- Black carbon (BC) transport has been observed between Santiago and a site in the Andes Mountains.
- BC transport is higher in summer than in winter.
- Transport is responsible for most BC observed in the mountain site.
- Travel time is about 9 h in winter and 11 h in summer.

ARTICLE INFO

Keywords:
Black carbon
Glaciers
Transport
Air pollution

ABSTRACT

Near Santiago de Chile and towards the Andes Mountains there are several areas sensitive to contamination, such as, the Natural Sanctuary Yerba Loca, National Park Rio Clarillo, several glaciers and the Farellones ski resort. The health of the glaciers is very important, because a large fraction of the water supply of Santiago is provided by them. To study the influence of Santiago's contamination on the glaciers, a black carbon monitoring campaign was performed from December 2014 (summer) until July 2015 (winter). Four monitors were placed between the city and the glaciers in the mountain along with meteorological stations. An analysis of the measurements indicates a direct transport of black carbon between Santiago de Chile and the Andes Mountains with a travel time of about 11 h in summer and 9 h in winter. Black carbon concentration at the mountain (La Parva) is higher in summer and lower in winter, a trend that is opposite to any other city in Chile. This is the only town in Chile in which transport, not local emissions, is mostly responsible for the BC observed. The fraction of BC in La Parva compared to Las Condes in the eastern part of Santiago changes from 14% in December to 2% in July. Model simulations of black carbon using high resolution meteorological data generated by a regional climate model confirms the difference in summertime and wintertime transport of black carbon from Santiago to La Parva. In December (summer) emissions from Santiago are estimated to contribute with 51% to the concentrations in La Parva while nearby sources from mining activities and long distance transport from other sources in central Chile contributes with 37 and 12% respectively. In July (winter) simulated contributions are dominated by long range transport from other sources with a 50% contribution while simulated contributions from sources in Santiago and from mining are both 25%. The contribution from mining activities is uncertain due to inaccuracies in simulated wind speed and direction in the mountains and too coarse model resolution and therefore warrants further investigation.

* Corresponding author.
E-mail address: egramsch@gmail.com (E. Gramsch).

https://doi.org/10.1016/j.atmosenv.2020.117546
Received 26 December 2019; Received in revised form 19 March 2020; Accepted 19 April 2020
Available online 24 April 2020

1. Introduction

Santiago de Chile is a relatively large city that has about 7 million inhabitants and it is located between two mountain ranges, the Andes on the east and the Coastal Range on the west. Like most cities surrounded by mountains, pollution levels in Santiago are very high in winter because of low wind speeds and strong temperature inversions (Gramsch et al., 2014). The climate is semi-arid with an annual precipitation of only 300 mm and the city relies strongly on water from the Andes coming from snow thaw and dams (Rutland and Garreaud, 1995). During summer, the water supply to the city comes mostly from several mountain glaciers on top of the Andes Mountains. A glacier inventory of the area (Marangunic, 1979; Peña and Nazarala, 1987; Rabatel et al., 2013) indicates a total of 154 glaciers, with an area of 67.6 km^2. Most glaciers are very small (area less than 1 km^2) and only 13 of those have areas between 1 and 9 km^2, the total water reserve from these glaciers was estimated in 3.38 km^3. The largest glaciers include: La Paloma, Olivares Alfa, Olivares Beta, Olivares Gamma, El Morado, Marmolejo, Esmeralda, Tronquitos, Juncal Norte, Juncal Sur, Risopatrón. Some of these glaciers (La Paloma, Olivares Alfa, Beta and Gamma) are located at close distance from one of the monitoring sites in La Parva. Continuous water supply from the glaciers is very important to the water supply of Santiago and the protected areas nearby such as, Natural Sanctuary Yerba Loca and National Park Rio Clarillo. It is also well documented that air pollution contributes to glaciers shrinking because black carbon (BC) strongly absorbs radiation accelerate melting of snow and ice (Painter et al., 2013; Ming et al., 2009; Yasunari et al., 2016; Thevenon et al., 2009; Maurer et al., 2019). The Andes Mountain glaciers are located between 50 and 100 km downwind from Santiago de Chile, thus a sizable fraction of the black carbon generated in the city is likely to be deposited on the surface of the glaciers (Cordoba et al., 2016; Cereceda-Balic at al., 2012; Molina, 2015). A recent study (Rowe et al., 2019) found that the average mass mixing ratio of BC in snow in the center of Chile was higher than in the north or south, confirming that sites closer to urban areas have higher impact from BC generated in cities. In this work, a six month campaign was performed in order to study the transport of black carbon from the city towards the mountains. Several instruments have been placed between the city and the glaciers in order to determine the time is takes for BC to reach the mountains. To further support the analysis, a chemistry transport model covering the central part of Chile was used to simulate the fate of black carbon emissions in the region.

2. Methods

2.1. Observations of black carbon and meteorological conditions

In this work the transport of BC has been studied from December of 2014 until July 2015 using instruments located in downtown Santiago (Usach), 500 m above sea level (m.a.s.l.); Las Condes, 795 m.a.s.l., towards the east of the city; Quiosco, at 1181 m.a.s.l., an intermediate site between Santiago and the glaciers; and La Parva, 2800 m.a.s.l., near the glaciers. La Parva is a ski resort that is inhabited mostly in the months of June, July and August. Fig. 1 shows the sampling sites as well as the location of the glaciers nearby.

BC Measurements were performed in La Parva, Usach and Quiosco with an optical instrument (SIMCA; Gramsch et al., 2004). At La Parva and Usach, meteorological stations were also installed to measure wind speed and direction, temperature, humidity, pressure and precipitation (NovaLynx, Grass Valley, CA, USA, model 110-WS-25). At Las Condes site, black carbon was measured with an Aethelometer (Magee Scientific, Berkeley, CA, USA, model AE33). This site belongs to the Ministry of the Environment and has instruments to measure $PM_{2.5}$, PM_{10}, gases and meteorology. Meteorological data from Parque O'Higgins station, also in the Ministry of Environment network, was used for comparisons to meteorological simulations. Both instruments use the same principle to measure BC that is, measuring the light absorption of the particles in the air, seeking to reduce the influence of light scattering on the measurement (Horvath, 1993).

The SIMCA uses a variation of the integrating plate method (Lin et al., 1973) to measure the absorption coefficient. In this method, a volume of air is drawn through a filter and particles with sizes bigger

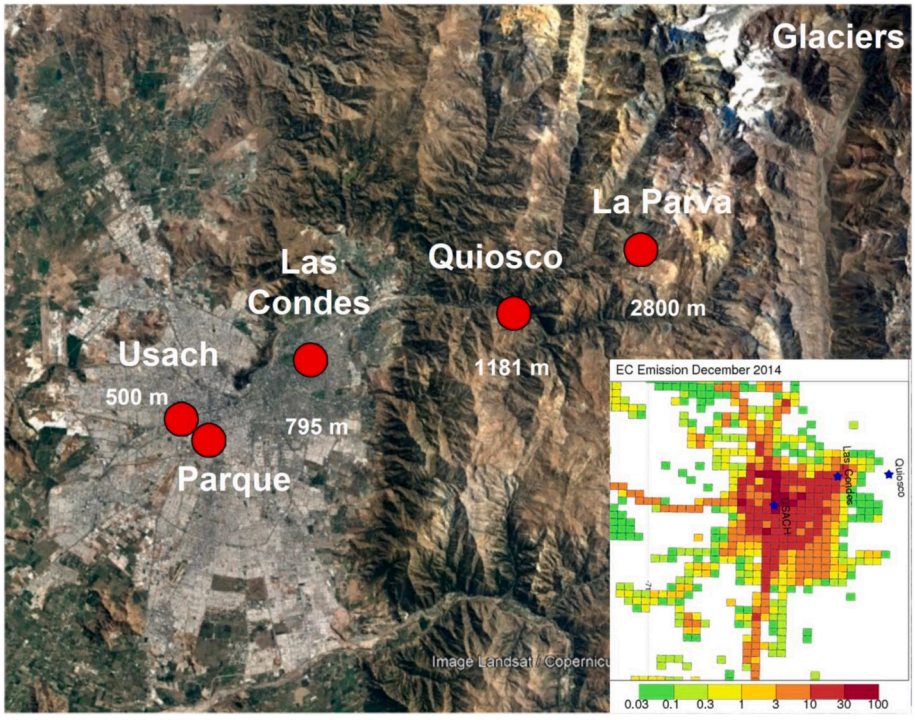

Fig. 1. Map of the study area with the location of the sampling sites. Usach and Las Condes are located inside Santiago de Chile. The inset shows the EC emission distribution in the Santiago region for December. Units: ton yr^{-1}.

than or similar to the pore size are collected. An LED is placed on one side of the filter, a photodetector on the other side, and the intensity of light that passes through the filter is measured. The measurements were made before and after the particles were collected. Without changing the filter, a new volume of air is drawn and new transmission measurements are made. This process allowed us to obtain the absorption coefficient over an extended period of time without changing the filter. However, several assumptions have to be made:

- The optical properties of the particles in the airborne state are the same as when they are in the filter.
- There are no multiple passes of light through the filter.
- Only the light absorbed by the particles is missing from the measurements. A special optical arrangement was built to ensure that scattered light is integrated and measured.
- The Lambert–Beer law for light absorption by particles is valid.
- The transmission properties of the filter do not vary as more particles are collected.

The SIMCA monitor collects particles in a filter by pumping air for 1 min every 15 min, however, to increase the sensitivity, the pumping time was increased to 2 min, in La Parva and Quiosco sites. Calibration of the optical monitors (Simcas) was carried out by running all equipment simultaneously with an EC-OC Sunset monitor (Sunset Laboratory, Tigard, OR, USA) for several days at Usach before the start of the campaign. The Aethalometer uses the same optical absorption principle, but it employs a continuous filter to measure the light absorption (Hansen et al., 1984).

2.2. Model set up for central Chile

In order to simulate the distribution and transport of emissions of black carbon over the Central part of Chile, the regional climate model HCLIM (Belušić (2020) has been used to simulate the meteorological conditions in the region with high spatial and temporal resolution. The output from HCLIM is then used to drive the MATCH atmospheric chemistry and transport model (Robertson et al. (1999) for simulation of the distribution of black carbon. The different geographical domains covered by the different models are shown in Fig. 2.

HCLIM was set up with two nested domains centered over central Chile with 12 and 3 km horizontal resolution (Fig. 2). The model had 65 levels between the surface and 10 hPa with 19 levels below 1 km. Boundary conditions for the outer 12 km domain were taken from the ERA-Interim (Dee et al., 2011) global reanalysis at six-hourly time intervals. HCLIM was run in climate mode without assimilation of local meteorological data for December 2014 and July 2015. Model output was stored with 1-h time resolution for use in MATCH.

The MATCH CTM has been used for simulation of the distribution of black carbon. MATCH has also been used previously to study sulphur air pollution in central Chile and arsenic dispersion from mining activities across Chile (Gallardo et al., 2002; Olivares et al., 2002; Gidhagen et al., 2002) as well as recently for PM2.5 and other criteria pollutants over the central part of Chile (Langner et al., 2020). This study is focused on black carbon and includs only primary anthropogenic emissions of black carbon in the model simulations using a model setup that otherwise is identical to the one used by Langner et al. (2020). The MATCH model was run on a 2 × 2 km horizontal grid resolution in order to utilize the available resolution in the emission data base.

Data on anthropogenic emissions were taken from the emission inventory developed by Usach (2014). The inventory includes different gaseous pollutants as well as primary emissions of $PM_{2.5}$ and PM_{10}. The emission data is valid for 2012 but here it is assumed that the information is valid also for 2014 and 2015. The inventory includes emissions from 12 different sectors. Total emissions of $PM_{2.5}$ for the central part of Chile for different sectors are given in Table 1. The emission inventory does not include the separation of primary $PM_{2.5}$ into different

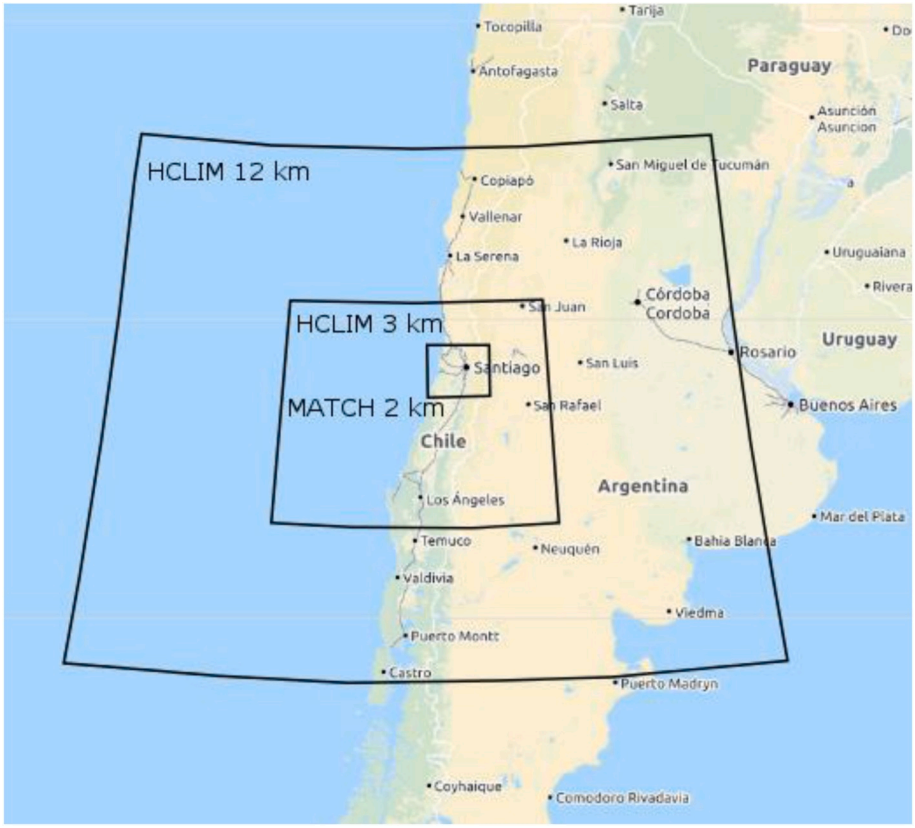

Fig. 2. Map of the different model domains used in the study. © OpenStreetMap contributors 2019. Distributed under a Creative Commons BY-SA License.

Table 1
PM2.5 emissions for 2012 used in the MATCH simulations. Units: ton/year.

Emission sector	$PM_{2.5}$
Stationary combustion and industrial processes	8300
Residential wood combustion	10 396
Field burning	1453
Wildfires	3439
Machinery	1095
Fugitive emissions	0
Road traffic light vehicles	903
Road traffic heavy vehicles	1632
Agriculture	33
Residential heating (excl. wood)	14
Resuspension	793
Biogenic	0
Sum	**28 058**

components of the aerosol. Therefore a simplified split of the PM emissions into elemental carbon (EC), organic material (OM) and other constituents ("dust") was assumed following Langner et al. (2020) (Table 2). The split is based on Kuenen et al. (2014), Akagi et al. (2011) and Reid et al. (2005). Hourly emissions reflecting seasonal, weekly and diurnal variations for different emission sectors were extracted from the emission data base as input to the MATCH CTM simulations.

3. Results

3.1. Simulated and measured wind pattern

Fig. 3a and Fig. 3b shows observed and simulated wind direction for the first half of December 2014 and July 2015 at the station Parque O'Higgins located in a park inside Santiago near the Usach sampling site. The night time periods are indicated with gray shaded boxes. In December the average observed wind direction is from south west (213°) indicating an influence of upslope winds towards the Andes mountain range. During some nights the wind direction turns to north and east indicating a nighttime downslope wind. The HCLIM model captures the average wind direction rather well (190°) but simulates winds in the north east sector during nighttime more frequently than observed resulting in a bias towards the south in the average. The average diurnal cycle of the wind speed for the same station is shown in Fig. 4a. In December there is a clear diurnal cycle with stronger winds during daytime. The timing of the diurnal cycle is well captured in the model simulation but winds are about 2 m/s too strong during midday. In July the observed wind direction has a stronger diurnal variability and the average direction is more from the south (176°). The model simulation also shows a pronounced diurnal variability in wind direction and the average simulated wind direction is also in the south to south east sector (154°). Both observed and simulated wind speeds are much lower in July, Fig. 4b, and the diurnal cycle is weak. Simulated wind speeds in July are about 0.5–1 m/s too strong with a daytime peak in the afternoon instead of during midday as in the observations.

Table 2
Split of primary PM emissions into elemental carbon (EC), organic matter (OM) and other (non-carbonaceous) components ("Dust") for different emission sectors, used in the MATCH simulations.

Emission sector	EC %	OM %	Dust %
Stationary combustion and industrial processes	7	7	86
Residential wood combustion	9	62	29
Field burning	6	87	7
Forest fires	4	87	9
Machinery	43	32	25
Road traffic light vehicles	29	53	17
Road traffic heavy vehicles	67	25	8
Agriculture	0	32	68
Residential heating (excl. wood)	10	90	0

Corresponding comparisons for La Parva in December are shown in Figs. 3c and 4c. The simulated wind direction is quite close to observed during daytime with a direction from the south west. During night the simulated direction is from the north west while the observed direction is more northerly or from north east. The diurnal variation in wind direction is close the observed one but the simulated wind speed is about 2–3 m/s too strong during both day and night. Saide et al. (2016) report similar biases in simulated surface wind speeds as found here for stations in central Chile using WRF as the meteorological model. They suggest that limited horizontal resolution, 2 km in their study, and lack of topographic and urban canopy parameterization could be the reason. Also, the topography in the vicinity of La Parva is very complex and it is not possible to fully represent this with the resolution used in HCLIM. Overall our conclusion is that the comparisons reported here indicate that HCLIM manages to capture the main differences in the wind regime between summer and winter in the study region even if details in wind speed and direction in the mountains are not possible to capture.

3.2. Black carbon observations and simulated transport

BC measurements took place between December 2014 and July 2015 in La Parva and Las Condes. Measurements in Quiosco were performed from February to July 2015. At the Usach site, BC measurements are performed continuously and data from December 2014 until September 2015 have been used. The average diurnal cycle based on hourly averages has been used to visualize the trends in the BC contamination at all stations. Fig. 5 shows the average diurnal cycle for each site for all months of the campaign, the night periods are highlighted with gray shaded boxes. It is very clear at the Usach and Las Condes sites that the BC concentration increases from December (summer) to July (winter) which is consistent with previous studies (Gramsch et al., 2004, 2006; Molina et al., 2017). During winter, low wind speeds and strong inversion, prevent the dispersion of contaminants, leading to high concentrations, especially at night. As a consequence, the highest concentrations are always seen in the months of May, June and July. It has to be noted that this trend is observed in all cities in Chile. At Usach, there is a distinct rush hour peak between 8 and 10 a.m. During the afternoon, BC concentration decreases because the wind speed and vertical turbulent mixing increases and there is less traffic. At night, there is an increase in concentrations due to rush hour and space heating emissions, the wind speed is low and the planetary boundary layer (PBL) is close to the ground, thus turbulent mixing is suppressed leading to accumulations of emissions (Gramsch et al., 2006, Gramsch et al., 2014). The BC average in Las Condes has a slightly different shape. BC concentration is less than half of what is observed at Usach, partly because the site is 300 m higher than Usach and the top of the thermal inversion during winter is at a lower altitude (Gramsch et al., 2014) and partly because of lower emissions. The rush hour peak in this site is not as pronounced as in Usach. An interesting feature of this site is the fact that during the afternoon (2–6 p.m.), in the winter months, BC concentration does not decrease as in Usach. This is an indication that the afternoon wind does not clean the area as in Usach, but carries pollution from Santiago's downtown into Las Condes. Fig. 5b shows a smaller peak between 1 and 3 p.m., which seems to be related to transport of BC from downtown Santiago. At night, in Las Condes, concentrations do not increase as in Usach mainly because there is thermally-driven downslope wind flow caused by differential heating during the day and night that comes down from the mountains bringing clean air to the area (Muñoz and Undurraga, 2009 and references therein, Gramsch et al., 2006). Synoptic-scale southerly jet events off central Chile occur year-round, but they are more frequent during spring–summer (over 60% of the time). Thus, during winter, there is less influence from synoptic-scale wind patterns (Garreaud and Muñoz, 2005).

The variation in concentrations and transport patterns seen in the observations are also evident in the model simulations. An example of model simulated transport in the region during the December 10, 2014

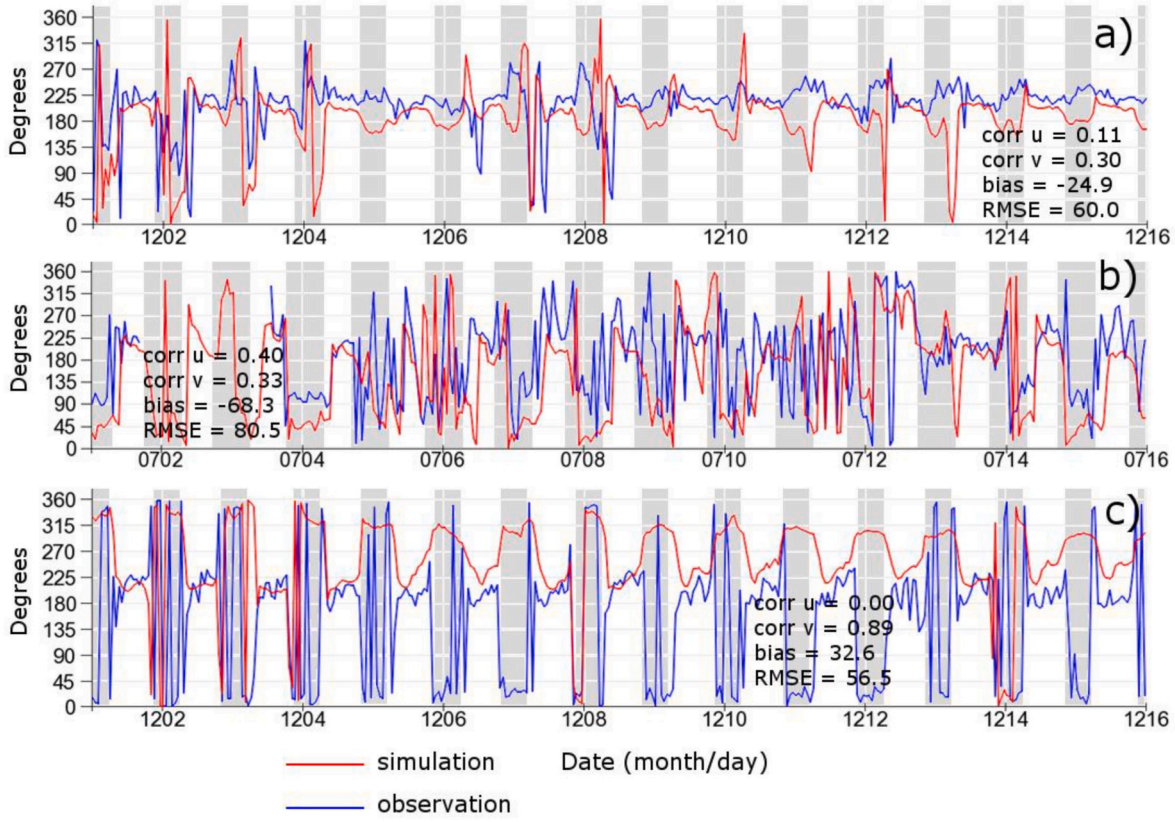

Fig. 3. Comparison between the measured wind direction (blue) and simulated by the HCLIM model (red) at: a) Parque O'Higgins for first half of December 2014 and b) July 2015 at La Parva and c) for first half of December 2014 at La Parva. The night periods are highlighted with gray shaded boxes. (For interpretation of the references to color in this figure legend, the reader is referred to the Web version of this article.)

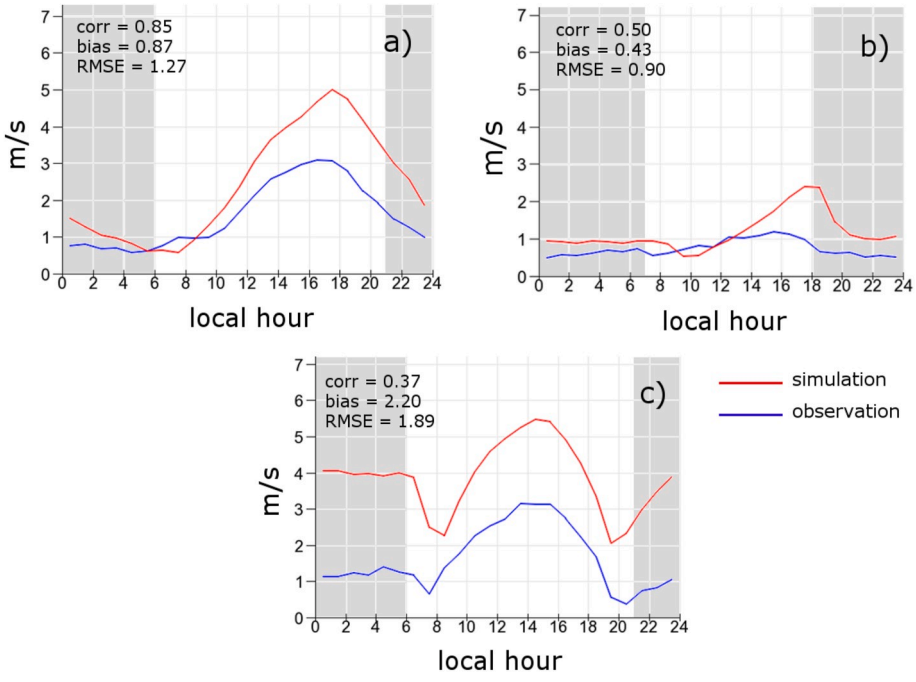

Fig. 4. Comparison between measured (blue) and simulated by the HCLIM model (red) average diurnal variation of the wind speed at: a) 10 m at Parque O'Higgins for December 2014, b) Parque O'Higgins for July 2015 and c) for La Parva in December 2014. The night periods are highlighted with gray shaded boxes. (For interpretation of the references to color in this figure legend, the reader is referred to the Web version of this article.)

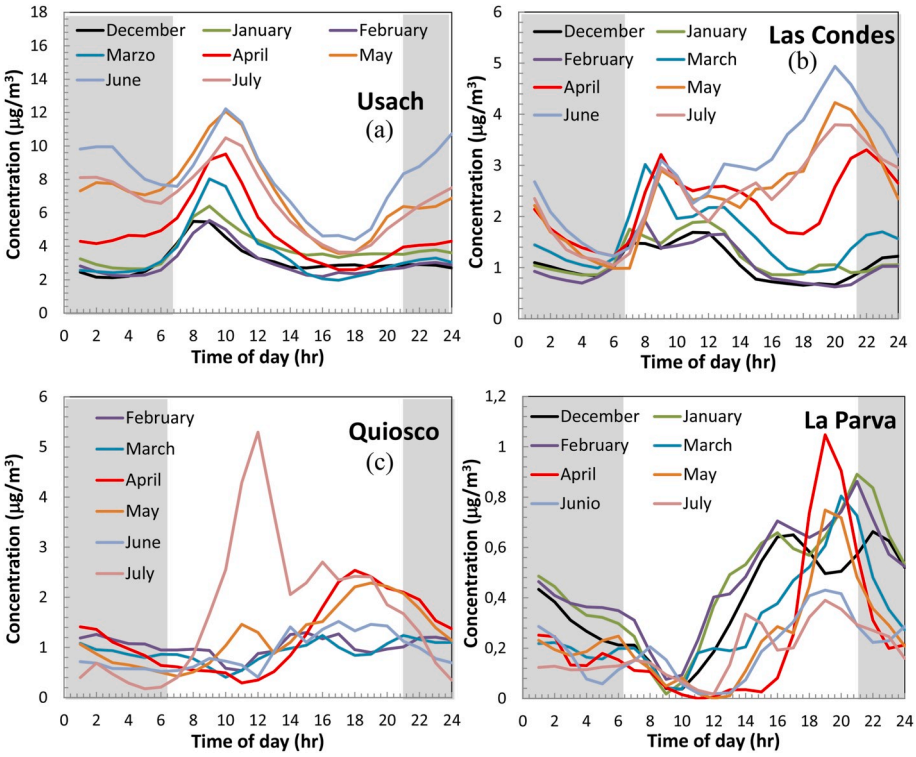

Fig. 5. Average diurnal cycles at the four sites for the months of December 2014 to July 2015. The night periods are highlighted with gray shaded boxes.

is given in Fig. 6 which shows vertical cross sections at 6 h intervals of simulated BC concentrations and winds along a transect from west to east aligned with the surface measurement stations. The location of the transect is indicated in Fig. 12. At 3 a.m. (Fig. 6a) the surface wind in Santiago is weak and easterly and along the mountain side up to the La Parva station the winds are also weak. Higher up on the Andes mountains winds are westerly, driven by the large scale synoptic circulation. Enhanced concentrations are simulated above the surface over Santiago in a residual layer that is due to vertical mixing of surface emissions during the previous day. Enhanced concentrations along the mountain side due to transport and mixing on the day before are also visible. At 9 a.m. (Fig. 6b) surface emissions in Santiago has started to build up and mix vertically. Surface winds in Santiago are still weak. Along the mountain side up to La Parva consistent westerly winds can be seen. At 3 p.m. (Fig. 6c) the wind is westerly throughout most of the cross section showing a clear example of thermally driven upslope winds. The emissions from Santiago are mixed vertically and transported towards the mountain range giving rise to increasing concentrations at Las Condes, Quiosco and La Parva. At 9 p.m. (Fig. 6d) the vertical turbulent mixing has ceased and the boundary layer has collapsed leaving a residual layer of high concentrations aloft over Santiago. The winds at the surface and in the lowest few hundred meters in Santiago are now easterly and air with low concentrations of BC are brought down from aloft and along the mountain side towards the city. Similar simulated concentration and transport patterns are found on most of the days in December 2014 with some variations due to varying synoptic conditions (not shown).

A polar graph with the wind speed, direction and BC concentrations at Las Condes is shown in Fig. 7. The plot shows the average for all months, with the brown color indicating higher and blue lower BC concentrations. It can be seen that the highest concentrations at Las Condes occur when the wind direction is S-W, i.e. from downtown towards Las Condes. In addition, higher concentrations are obtained when wind speed is greater than 1–2 m/s, which indicates that BC is not generated locally but comes from longer distances (downtown Santiago).

In Quiosco (Fig. 5c), no rush hour peak is seen during the morning because this site is outside of the city with very little traffic. However, there is a large peak in July, which is related to traffic from Santiago towards La Parva during the ski season. At this site, an increase in BC can be noticed during the afternoon and evening for all months, which is most likely related to transport of BC from the city. At night (10–12 p.m.) there is a decrease in concentrations, with is related to the thermally driven downslope flow that comes down from the mountains.

In La Parva, like in Quiosco, there is no traffic in the morning and no rush hour peak is seen (Fig. 5d). But in the afternoon and evening an increase in BC is clearly seen. This increase is different for the summer (December–March) and fall/winter (April–July) months. During warmer months, the increase in BC starts around 10–12 a.m. and the concentration during the afternoon is higher than in winter months at the same time. In winter, the increase in BC starts at 3–5 p.m. The difference in shape is an indication that transport of pollution changes with the season. A polar graph with wind speed, direction and BC concentrations in La Parva is shown in Fig. 8. As before, the brown color indicates higher BC concentration. The plot is very similar to Las Condes, i.e. the highest concentrations occur with S-W wind direction i.e. coming from the city. At La Parva, higher concentrations arise when wind speeds are greater than ~3 m/s which indicate that BC also comes from large distances. In this site, there are two competing processes, higher wind speeds and shorter transport time, reduce the time available for turbulent dilution – contributing to higher concentrations. On the other hand mechanical mixing associated with higher wind speeds could enhance dilution leading to lower concentrations. Both processes contribute to the measured concentrations but can be seen when wind speeds are higher than ~3 m/s. There are two local sources of BC towards north-east of La Parva, which are Los Bronces and Andina copper mines. BC concentrations from these mines can be seen in Fig. 11 as a small region with higher concentrations. However, the measurements (Fig. 8) seem to show that there is very little BC transport from the mines to La Parva because the polar plot shows a very small increase when the wind comes from the north-east.

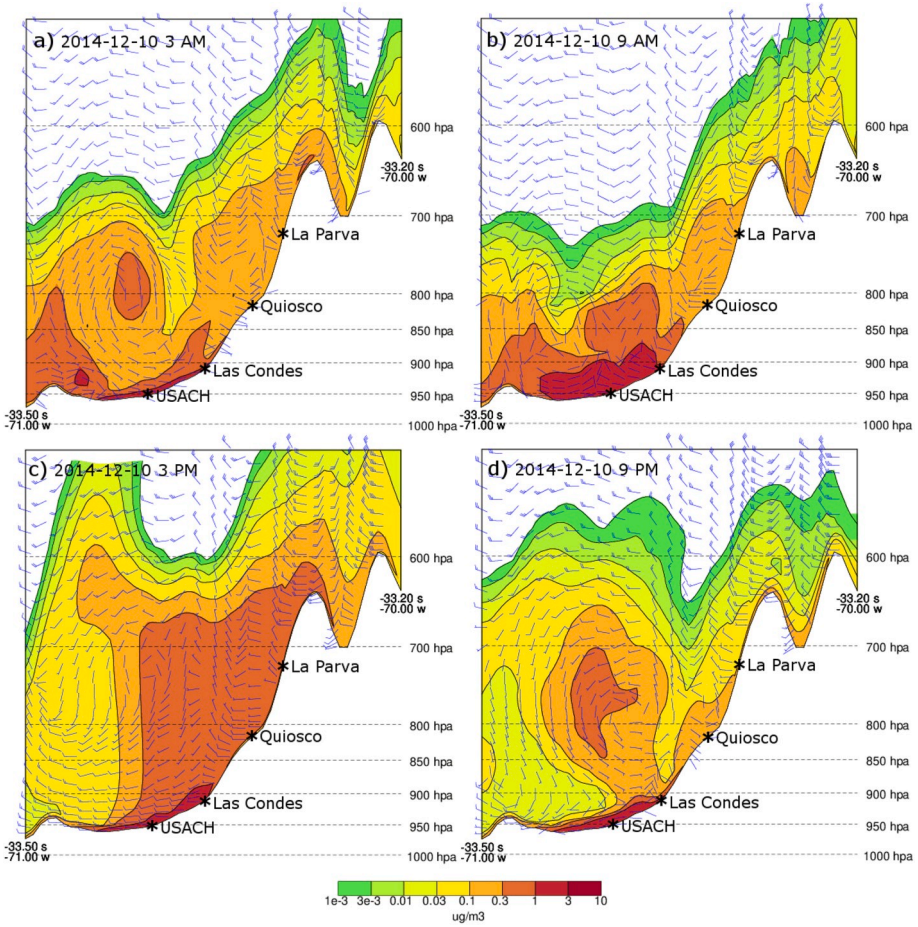

Fig. 6. Vertical cross section of simulated BC concentrations and winds along a transect aligned with the BC surface observations stations. Results are shown for 10 December at a) 3 a.m., b) 9 a.m., c) 3 p.m. and d) 9 p.m.. The location of the transect is indicated in Fig. 12. The wind barbs indicate wind direction and wind speed parallel to the plane of the cross section.

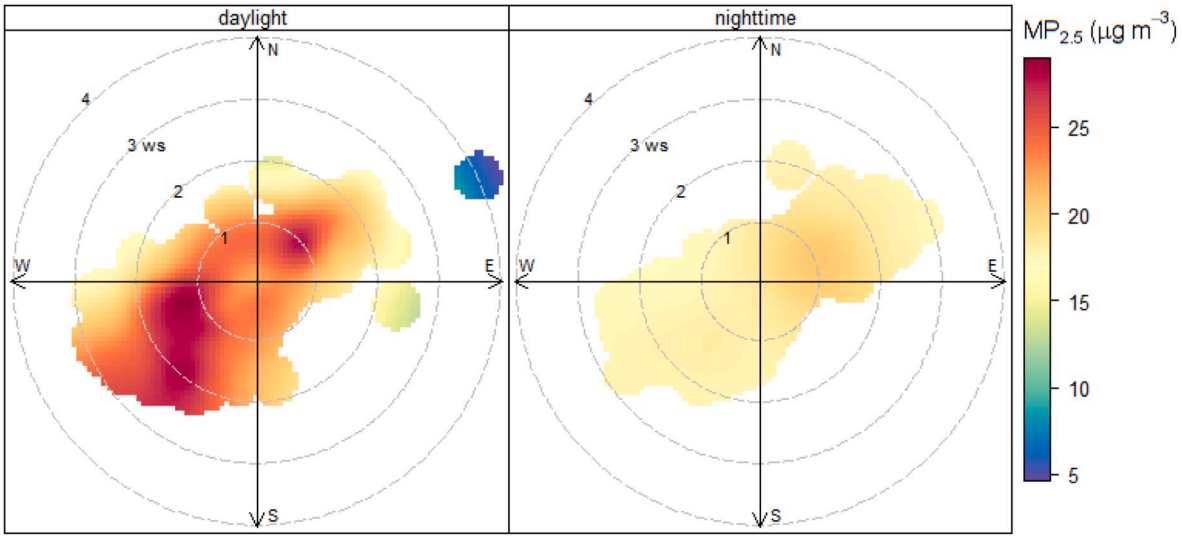

Fig. 7. Polar graph in Las Condes for BC concentration, windspeed and direction for all data (December 2014 to July 2015). The left pane shows the daytime hours (10 a.m.–7 p.m.) and the right pane shows nighttime hours (8 p.m.–9 a.m.).

3.3. BC transport

Another indication that transport of contaminants can be seen from the city towards the mountains can be seen in Fig. 9, with monthly average plots for March (summer) and July (winter) for all stations. The maximum BC concentration in downtown Santiago (Usach site) is reached at ~ 9 a.m. in March and ~10 a.m. in July, indicated with (1) in the figure. At Las Condes, there is a secondary peak at ~1 p.m. in March

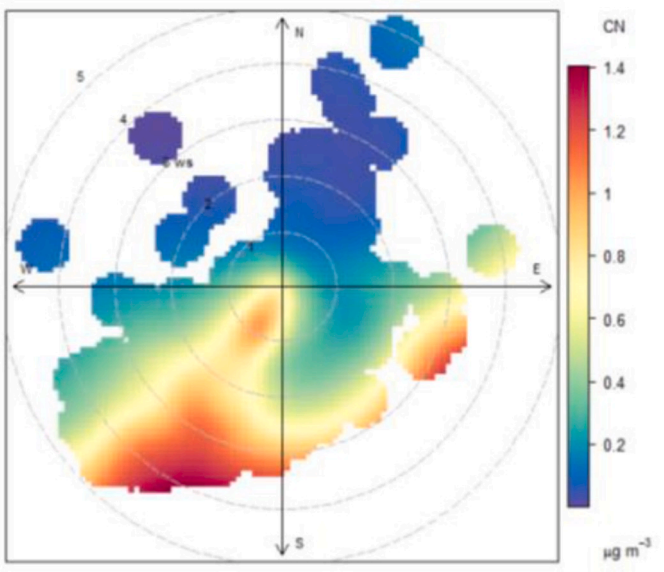

Fig. 8. Polar graph for BC concentration, wind speed and direction for all data in La Parva (December 2014 to July 2015) for daytime hours (10 a.m.–7 p.m.).

and about 3 p.m. in July, indicated with (2). In the intermediate site (Quiosco) there is a BC maximum at ~ 4 p.m. in March and ~6 p.m. in July, indicated with (3). At La Parva, the BC maximum is reached at ~8 p.m. in March and ~7 p.m. in July. The plots show a BC peak that starts in downtown Santiago at ~9 a.m. and moves east, reaching La Parva at ~8 p.m. For the other months, there is a similar displacement of the BC curve towards the mountain.

The monthly average for the whole period for all stations is shown in Fig. 10a. Several features can be clearly seen, which are mostly related to the meteorology and topography of the sampling sites. The highest BC concentrations are observed at the Usach site, which is located near downtown Santiago. The BC concentration in winter is more than two times the concentration in summer. The open triangles are the MATCH-model simulated concentrations at Usach and the open circles are the results in Las Condes for December 2014 and July 2015. Lower concentrations are measured at Las Condes, located on the eastern side of the city and almost 300 m higher. It is well known that high BC levels are encountered in the center of the city, because of the high traffic emissions from diesel vehicles, space heating from wood stoves and low wind speeds (Trier et al., 1997; Gramsch et al., 2006). As mentioned before, Las Condes site has lower BC concentrations because it has less traffic and because there is a thermally driven downslope wind flow coming from the mountains that cleans the atmosphere in the afternoon (Gramsch et al., 2014). The subsidence thermal inversion (Rutland and Garreaud, 1995; Muñoz et al., 2009), coupled to frequent surface inversions that occur in winter, can explain the decreasing BC concentrations that are observed as the altitude increases. BC concentrations in Quiosco at 1181 m.a.s.l. are lower than at Las Condes and Usach. The lowest concentrations are found in La Parva, at the highest altitude, 2800 m.a.s.l. However, a very interesting feature can be extracted from Fig. 10b; the BC concentration in La Parva decreases in winter. This trend is opposite to what is observed in the other stations and opposite to all other cities in Chile (Molina et al., 2017), in which the highest concentrations are found in winter, not summer. This is an indication that most BC found in La Parva originates in Santiago and is transported to the mountains. This is the only town in Chile in which transport, not local emissions, is totally responsible for the BC observed. Because in winter the thermal inversion is at lower altitude and upslope winds are weaker, BC particles are inhibited to move towards La Parva. The fraction of BC that is transported from Las Condes to La Parva can be estimated from a comparison of the monthly average. The fraction of BC in La Parva compared to Las Condes changes from 14% in December to 2% in July.

3.4. Simulated average BC concentrations and source contributions

Fig. 11 shows average BC concentrations for December 2014 and July 2015 simulated by the MATCH model. In line with the observations, simulated concentrations are about a factor of two higher in July than in December in the whole region from Santiago and to the west. As in the observations the highest concentrations in Santiago are simulated in the city center close to the Usach station with a gradient towards lower concentrations at Las Condes and up towards the mountains. Apart from inside Santiago enhanced concentrations of black carbon are simulated in connection with other urban areas in the region and in the vicinity of industrial sources found mainly around Santiago and in the north western part of the model domain. The highest concentrations are simulated in July in the city of Rancagua to the south of Santiago and are related to high emissions from wood burning in winter (Gramsch et al., 2004). The local maximum in the mountains to the north of La Parva originates from mining activities in the area.

The model simulated results are compared to monthly average observations in Fig. 10a. The simulated concentrations agree quite well with the observations from the stations in Santiago (Usach and Las Condes). Both, the difference between summer and winter and the difference in concentration levels between Usach, close to the city center, and Las Condes, to the east, is captured in the model simulation. At the stations in the mountains the model simulates lower concentrations than observed. There could be several reasons for this, including missing local emission sources, inaccuracies in the simulated thermally driven upslope transport from Santiago, inaccuracies in the simulated vertical mixing and inaccuracies in the wind simulation in Quiosco and La Parva. Fig. 10b shows the results for Las Condes and La Parva in more detail. Although simulated concentrations are lower than observed at La Parva the observed feature of an opposite trend in concentrations between summer and winter between the two stations is well captured by the

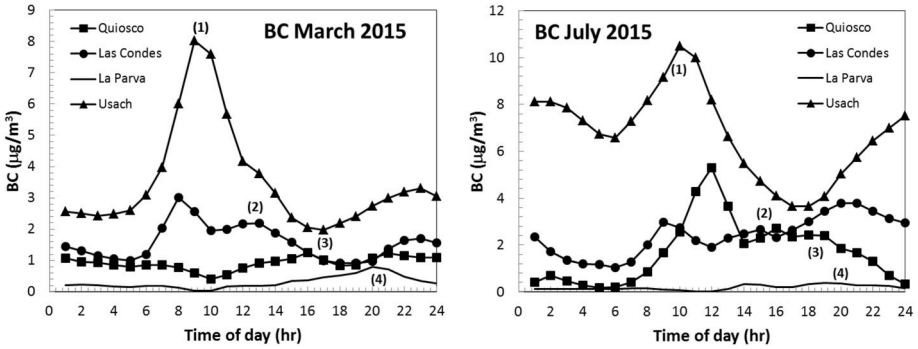

Fig. 9. Monthly BC average for March (summer) and July (winter) at the four stations.

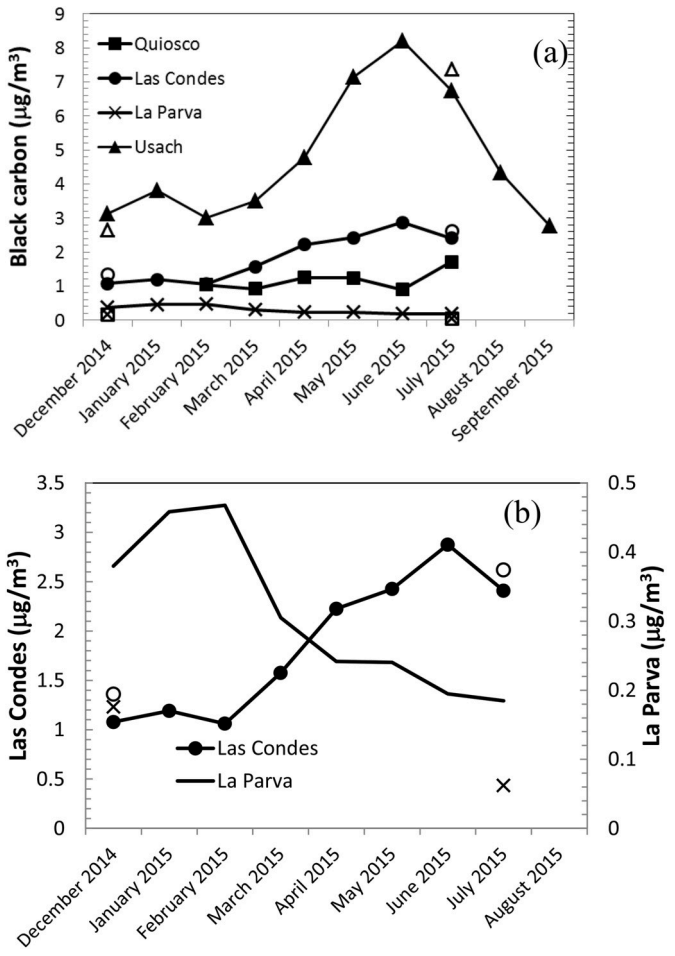

Fig. 10. (a) Monthly average black carbon concentration for all sites. (b) Montly BC average for Las Condes and La Parva. The open triangles are the simulated results for Usach, open circles for Las Condes, open squares for Quiosco and crosses for La Parva.

model.

To shed further light on the origin of BC at the different monitoring stations two additional model simulations were performed. In the first simulation all emissions in a rectangular area enclosing Santiago and suburbs (see Fig. 11) was set to zero. This simulation gives the contribution of all sources outside Santiago to the simulated concentrations. This contribution is named "Outside Santiago". The difference between the base simulation with all emissions and this simulation gives the contribution from Santiago emissions. This difference is named "Santiago". In the second simulation the emissions in the mining area to the north of La Parva were set to zero. The difference between the base simulation and this simulation gives the contribution from the mining area and this difference is named "Mining". Finally the contribution from other sources excluding mining and Santiago is given by the difference between the contributions from "Outside Santiago" and "Mining". This contribution is named "Other". Fig. 12 shows the percentage contributions from different sources to the concentrations at Quiosco and La Parva in December 2014 and July 2015. The contribution from Santiago is largest at both locations in December (summer) with 58% at Quiosco and 51% at La Parva. The second most important source in the model simulations for December is "Mining" with contributions of 24 and 37% while "Other" sources in central Chile contributes 18 and 12%

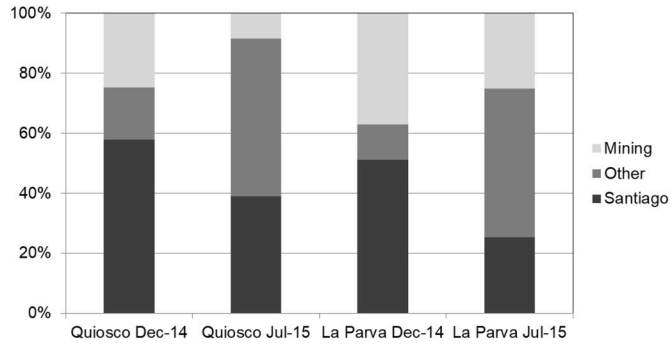

Fig. 12. Model simulated monthly average percentage contributions to surface concentrations from emissions in the area of Santiago, "Santiago", from mining activities in the Andes mountains north of La Parva, "Mining" and from the remaining sources in the central Chile inside the model domain, "Other", at the stations Quiosco and La Parva in December 2014 and July 2015.

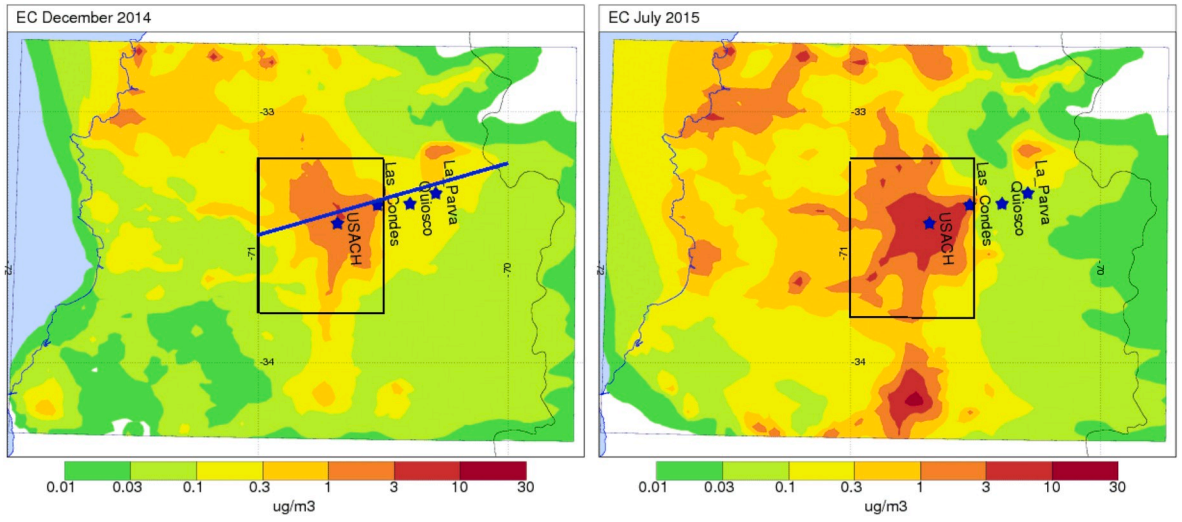

Fig. 11. Monthly average concentrations of black carbon simulated by the MATCH model for December 2014 (left) and July 2015 (right). Locations of the monitoring sites for black carbon are indicated by blue stars. The rectangular area around Santiago indicates the region inside which emission are coming from Santiago in the sensitivity simulations. The blue line indicates the position of the cross section presented in Fig. 6. Units: µg/m^3. (For interpretation of the references to color in this figure legend, the reader is referred to the Web version of this article.)

at Quiosco and La Parva respectively. In July (winter) the simulated contribution from Santiago is reduced to 39% at Quiosco and 25% at La Parva. Contributions from the mining area are also reduced to 8 and 25%. Instead the dominating contribution is from "Other" sources in central Chile excluding the Santiago area and the mining area with contributions of 53 and 50% for Quiosco and La Parva respectively. In July (winter) more distant sources from the whole of central Chile are dominating but at the same time the absolute concentrations at La Parva are lower. These results further support the hypothesis that much of the black carbon that is observed in La Parva during summer originates from Santiago. Given that simulated concentrations at La Parva are lower than observed the contribution from Santiago could be higher in reality than simulated by the model. The mining activities to the north of La Parva give a substantial contribution in December (summer) in the model simulations. Given the complex topography in the region, the limited model resolution, and the biases seen in modeling the observed winds at La Parva the simulated size of this contribution must be considered uncertain and warrants further investigation. The observations of BC in La Parva (Fig. 8) indicating a small influence of transport from the mining areas further supports this assessment.

4. Conclusions

Black carbon has been measured continuously for 8 months at 4 sites between Santiago de Chile and the Andes mountains, and the diurnal profiles of each site shows features related to its location. The black carbon profile for Usach in downtown Santiago shows influence mainly from local sources (traffic, space heating, etc.). In Las Condes, towards the east of the city, there is a mixed influence from local sources and transport. In a site between the city and the mountains there is also a mixed influence, but in La Parva (in the mountains, close to the glaciers) most of the BC in summer is due to transport from Santiago. A comparison of the BC hourly average during March for all sites shows a peak that starts in downtown Santiago at ~9 a.m. and moves east; reaching La Parva at ~8 p.m. Polar plots show that in las Condes, the highest BC concentration is reached when the wind speed is higher than 1–2 m/s with a S-W direction. In La Parva, the highest concentration is reached with wind speeds higher than 3 m/s, also with an S-W direction. An interesting feature of the data is that the BC concentration in La Parva decreases in winter. This trend in is opposite to any other city in Chile, in which the highest concentrations are found in winter, not summer. The fraction of BC that is transported from Las Condes to La Parva can be estimated from a comparison of the monthly average. The fraction of BC in La Parva compared to Las Condes changes from 14% in December to 2% in July.

Model simulations of black carbon using high resolution meteorological data generated by a regional climate model confirms the difference in summertime and wintertime transport of black carbon from Santiago to La Parva. In December (summer) emissions from Santiago are estimated to contribute with 51% to the concentrations in La Parva while nearby sources from mining activities and long distance transport from other sources in central Chile contributes 37 and 12% respectively. In July (winter) simulated contributions are dominated by long range transport from other sources with a 50% contribution while contributions from sources in Santiago and from mining are both 25%. Given that model simulated concentrations at La Parva are underestimated the contribution from emissions in Santiago cold be underestimated both in summer and in winter. The contribution from nearby mining activities is uncertain due to inaccuracies in simulated wind speed and direction in the mountains and too coarse model resolution and therefore warrants further investigation.

Declaration of competing interest

The authors declare that they have no known competing financial interests or personal relationships that could have appeared to influence the work reported in this paper.

CRediT authorship contribution statement

Ernesto Gramsch: Conceptualization, Methodology, Writing - original draft. **Alicia Muñoz:** Data curation. **Joakim Langner:** Methodology. **Luis Morales:** Software, Validation. **Cristian Soto:** Data curation. **Patricio Pérez:** Visualization. **María A. Rubio:** Visualization.

Acknowledgement

This work was supported by Fondecyt projects 1151117 and 1170456. Lars Gidhagen at SMHI is gratefully acknowledged for help with the analyses of the HCLIM model simulations and Danijel Belušić and David Lindstedt are gratefully acknowledged for help with setting up the HCLIM model simulations.

Appendix A. Supplementary data

Supplementary data to this article can be found online at https://doi.org/10.1016/j.atmosenv.2020.117546.

References

Yasunari, T.J., Bonasoni, P., Laj, P., Fujita, K., Vuillermoz, E., Marinoni, A., Cristofanelli, P., Duchi, R., Tartari, G., Lau, K.-M., 2016. Estimated impact of black carbon deposition during pre-monsoon season from Nepal Climate Observatory – pyramid data and snow albedo changes over Himalayan glaciers. Atmos. Chem. Phys. 10, 6603–6615.

Akagi, S.K., Yokelson, R.J., Wiedinmyer, C., Alvarado, M.J., Reid, J.S., Karl, T., Crounse, J.D., Wennberg, P.O., 2011. Emission factors for open and domestic biomass burning for use in atmospheric models. Atmos. Chem. Phys. 11, 4039–4072. https://doi.org/10.5194/acp-11-4039-2011.

Belušić, et al., 2020. HCLIM38: a flexible regional climate model applicable for all climate zones. Geosci. Model Dev. (GMD) 13, 1311–1333. https://doi.org/10.5194/gmd-2019-151.

Cereceda-Balic, F., Palomo-Marín, M., Bernalte, E., Vidal, V., Christie, J., Fadic, X., Guevara, J.L., Miro, C., Pinilla-Gil, E., 2012. Impact of Santiago de Chile Urban Atmospheric Pollution on Anthropogenic Trace Elements Enrichment in Snow Precipitation at Cerro Colorado, Central Andes. Atmos. Environ. 47, 51–57.

Córdova, A.M., Arévalo, J., Marín, J.C., Baumgardner, D., Raga, G.B., Pozo, D., Ochoa, C. A., Rondanelli, R., 2016. On the transport of urban pollution in an Andean mountain valley. Aerosol Air Qual. Res. 16, 593–605.

Dee, D.P., Uppala, S.M., Simmons, A.J., Berrisford, P., Poli, P., Kobayashi, S., Andrae, U., Balmaseda, M.A., Balsamo, G., Bauer, P., Bechtold, P., Beljaars, A.C.M., van de Berg, L., Bidlot, J., Bormann, N., Delsol, C., Dragani, R., Fuentes, M., Geer, A.J., Haimberger, L., Healy, S.B., Hersbach, H., Hólm, E.V., Isaksen, L., Kållberg, P., Köhler, M., Matricardi, M., McNally, A.P., Monge-Sanz, B.M., Morcrette, J.-J., Park, B.-K., Peubey, C., de Rosnay, P., Tavolato, C., Thépaut, J.-N., Vitart, F., 2011. The ERA-Interim reanalysis: configuration and performance of the data assimilation system. Q. J. R. Meteorol. Soc. 137 (656), 553–597. https://doi.org/10.1002/qj.828.

Gallardo, L., Olivares, G., Langner, J., Aarhus, B., 2002. Coastal lows and sulfur air pollution in Central Chile. Atmos. Environ. 36, 3829–3841.

Garreaud, René, Muñoz, Ricardo, 2005. The low-level jet off the west coast of subtropical south America: structure and variability. Mon. Weather Rev. 133, 2246–2261.

Gidhagen, L., Schmidt-Thomé, P., Kahelin, H., Johansson, C., 2002. Anthropogenic and natural levels of arsenic in PM10 in central and northern Chile, Atmos. Environ. Times 36, 3803–3817. https://doi.org/10.1016/S1352-2310(02)00284-4.

Gramsch, E., Ormeño, I., Palma, G., Cereceda, F., Oyola, P., 2004. Use of the Light absorption coefficient to monitor elemental carbon and PM2.5 example of Santiago de Chile. J. Air Waste Manag. Assoc. 54, 799–808.

Gramsch, E., Cáceres, D., Oyola, P., Reyes, F., Vásquez, Y., Rubio, M.A., Sánchez, G., 2014. Influence of surface and subsidence thermal inversion on PM2.5 and black carbon concentration. Atmos. Environ. 98, 290–298.

Gramsch, E., Cereceda-Balic, F., Oyola, P., von Baer, D., 2006. Examination of pollution trends in Santiago de Chile with cluster analysis of PM10 and Ozone data. Atmos. Environ. 40, 5464–5475.

Hansen, A.D.A., Rosen, H., Novakov, T., 1984. The aethalometer—an instrument for the real-time measurement of optical absorption by aerosol particles. Sci. Total Environ. 36, 191–196.

Horvath, H., 1993. Atmospheric light absorption: a review. Atmos. Environ. 27, 293–317.

Kuenen, J.J.P., Visschedijk, A.J.H., Jozwicka, M., Denier van der Gon, H.A.C., 2014. TNO-MACC_II emission inventory; a multi-year (2003–2009) consistent high-resolution European emission inventory for air quality modelling. Atmos. Chem. Phys. 14, 10963–10976. https://doi.org/10.5194/acp-14-10963-2014.

Langner, J., Gidhagen, L., Bergström, R., Gramsch, E., Oyola, P., Reyes, F., Segersson, D., Aguilera, C., 2020. Model simulated source contributions to PM2.5 in Santiago and

in the central region of Chile. Aerosol Air Qual. Res. https://doi.org/10.4209/aaqr.2019.08.0374.
Lin, C.I., Baker, M.B., Charlson, R.J., 1973. Absorption coefficient of the atmospheric aerosol: a method for measuring. Appl. Optic. 12, 1356–1363.
Marangunic, C., 1979. Glacier Inventory in the Maipo Basin. General Water Management. https://snia.mop.gob.cl/sad/GLA1046v1.pdf. last visited April, 2020.
Maurer, J.M., Schaefer, J.M., Rupper, S., Corley, A., 2019. Acceleration of ice loss across the Himalayas over the past 40 years. Sci. Adv. 5 (6) eaav 7266.
Ming, J., Xioa, C., Cachier, H., Qin, D., Qin, X., Li, Z., Pu, J., 2009. Black Carbon (BC) in the snow of glaciers in west China and its potential effects on albedos. Atmos. Res. 92, 114–123.
Molina T, Luisa, et al., Luisa T. Molina, Laura Gallardo,M. Andrade, D. Baumgardner,M. Borbor-Córdova, R. Bórquez, G. Casassa, F. Cereceda-Balic, L. Dawidowski, R. Garreaud, N. Huneeus, F. Lambert, J.L.McCarty, J.Mc Phee,M.Mena-Carrasco, G.B. Raga, C. Schmitt, and J.P. Schwarz, 2015. Pollution and its Impacts on the South American Cryosphere. AGU Publications, Earth's Future 3, 1–25. https://doi.org/10.1002/2015EF000311. In press.
Molina, Carolina, Toro, Richard, Morales, Raúl G.E., Manzano, Carlos, Manuel, A., Leiva-Guzmán, 2017. Particulate matter in urban areas of south-central Chile exceeds air quality standards. Air Qual. Atmos Health 10 (5), 653–667.
Muñoz, R., Undurraga, A., 2009. Daytime mixed layer over the santiago basin: description of two years of observations with a Lidar ceilometer. J. Appl. Climatol. Meteorol. 49, 1728–1741.
Olivares, G., Gallardo, L., Langner, J., Aarhus, B., 2002. Regional dispersion of oxidized sulfur in Central Chile. Atmos. Environ. 36, 3819–3828.
Painter, T.H., Flanner, M.G., Kaser, G., Marzeion, B., VanCuren, R.A., Abdalati, W., 2013. End of the little ice age in the Alps forced by industrial black carbon. Proc. Natl. Acad. Sci. U.S.A. 110 (38), 15216–15221.
Peña, H., Nazarala, B., 1987. Snowmelt-runoff simulation model of a central Chile Andean basin with relevant orographic effects. In: Large Scale Effects of Seasonal Snow Cover, vol. 166. IAHS Publ.
Rabatel, A., et al., 2013. Current state of glaciers in the tropical Andes: a multi-century perspective on glacier evolution and climate change. Cryosphere 7, 81–102.
Reid, J.S., Koppmann, R., Eck, T.F., Eleuterio, D.P., 2005. A review of biomass burning emissions part II: intensive physical properties of biomass burning particles. Atmos. Chem. Phys. 5, 799–825. https://doi.org/10.5194/acp-5-799-2005.
Robertson, L., Langner, J., Engardt, M., 1999. An Eulerian limited-area atmospheric transport model. J. Appl. Meteorol. 38.
Rowe, P.M., Cordero, R.R., Warren, S.G., Stewart, E., Doherty, S.J., Pankow, A., Schrempf, M., Casassa, G., Carrasco, J., Pizarro, J., MacDonell, S., Damiani1, A., Lambert, F., Rondanelli1, R., Huneeus, N., Fernandoy, F., Neshyba, S., 2019. Black Carbon and Other Light Absorbing Impurities in Snow in the Chilean Andes, vol. 9, p. 4008. https://doi.org/10.1038/s41598-019-39312-0.
Rutland, J., Garreaud, R., 1995. Meteorological air-pollution potential for Santiago, Chile—towards an objective episode forecasting. Environ. Monit. Asses. 34 (3), 223–244.
Saide, P.E., Mena-Carrasco, M., Tolvett, S., Hernandez, P., Carmichael, G.R., 2016. Air quality forecasting for winter-time PM2.5 episodes occurring in multiple cities in central and southern Chile. J. Geophys. Res. Atmos. 121, 558–575. https://doi.org/10.1002/2015JD023949.
Thevenon, F., Anselmetti, F.S., Bernasconi, S.M., Schwikowski, M., 2009. Mineral dust and elemental black carbon records from an Alpine ice core (Colle Gnifetti glacier) over the last millennium. J. Geophys. Res. 114, D17102.
Trier, A. N. Cabrini, Ferrer, J., 1997. Correlations between urban atmospheric light extinction and fine particle mass concentrations. Atmósfera 10, 151–160.
Usach, U., 2014. Informe final: Actualización y sistematización del inventario de emisiones de contaminantes atmosféricos en la Región Metropolitana. Emission Inventory Final Report. Universidad de Santiago de Chile.